

# Raman spectra evidence for the covalent-like quasi-bonding between exfoliated MoS<sub>2</sub> and Au films

Xinyu HUANG<sup>1,2†</sup>, Lei ZHANG<sup>1,3†</sup>, Liwei LIU<sup>4\*</sup>, Yang QIN<sup>1,5</sup>, Qiang FU<sup>1,6</sup>,  
Qiong WU<sup>1,3</sup>, Rong YANG<sup>1</sup>, Jun-Peng LV<sup>6</sup>, Zhenhua NI<sup>6</sup>, Lei LIU<sup>2\*</sup>, Wei JI<sup>7</sup>,  
Yeliang WANG<sup>4</sup>, Xingjiang ZHOU<sup>1</sup> & Yuan HUANG<sup>1,8\*</sup>

<sup>1</sup>*Institute of Physics, Chinese Academy of Sciences, Beijing 100190, China;*

<sup>2</sup>*Department of Materials Science and Engineering, College of Engineering, Peking University, Beijing 100871, China;*

<sup>3</sup>*College of Materials Science and Engineering, Key Laboratory of Advanced Functional Materials, Ministry of Education of China, Beijing University of Technology, Beijing 100124, China;*

<sup>4</sup>*School of Information and Electronics, MIIT Key Laboratory for Low-Dimensional Quantum Structure and Devices, Beijing Institute of Technology, Beijing 100081, China;*

<sup>5</sup>*School of Science, Beijing University of Posts and Telecommunications, Beijing 100876, China;*

<sup>6</sup>*School of Physics, Southeast University, Nanjing 211189, China;*

<sup>7</sup>*Department of Physics and Beijing Key Laboratory of Optoelectronic Functional Materials & Micro-Nano Devices, Renmin University of China, Beijing 100872, China;*

<sup>8</sup>*Songshan Lake Materials Laboratory, Dongguan 523808, China*

Received 25 November 2020/Revised 19 January 2021/Accepted 21 January 2021/Published online 8 March 2021

**Abstract** Gold-enhanced mechanical exfoliation method attracts broad interests in recent years, which has been widely used for preparing large-area and high-quality 2D single crystals. Even many calculations predict that there is strong interaction between Au film and the exfoliated 2D crystals, direct experimental evidence is still lacking. Here, we perform Raman spectroscopy measurements for few layer MoS<sub>2</sub> with and without Au film underneath. The main peaks of MoS<sub>2</sub> on Au film show no obvious change at higher frequency, however, the breathing and shear modes at low-frequency are suppressed, especially for breathing modes. In contrast, both breathing modes and shear modes can be detected on suspended MoS<sub>2</sub> and the samples are transferred from Au film to SiO<sub>2</sub>/Si. These comparison results provide direct evidence for the existence of covalent-like quasi-bonding at the interface of Au film and the exfoliated MoS<sub>2</sub> crystal. This MoS<sub>2</sub>/Au interface interaction presents a special pinning-effect for low-frequency rigid vibration. Similar pinning-effect is also discovered in WS<sub>2</sub>/Au system. Our work reports the suppression of low-frequency Raman modes of MoS<sub>2</sub>, WS<sub>2</sub> on Au film, which will deliver new inspiration for studying other interactions between layered materials and solid surfaces.

**Keywords** MoS<sub>2</sub>, Raman spectroscopy, gold-enhanced mechanical exfoliation, low-frequency raman modes, covalent-like quasi-bonding

**Citation** Huang X Y, Zhang L, Liu L W, et al. Raman spectra evidence for the covalent-like quasi-bonding between exfoliated MoS<sub>2</sub> and Au films. *Sci China Inf Sci*, 2021, 64(4): 140406, <https://doi.org/10.1007/s11432-020-3173-9>

## 1 Introduction

Two-dimensional (2D) materials, in present of graphene and MoS<sub>2</sub>, have stimulated the fast progress in condensed matter physics and material sciences. Comparing with 3D layered materials, 2D counterparts show unique mechanical [1, 2], optical [3, 4] and electrical properties [5–7], and compatible with traditional Si-based in-plane fabrication technology [8, 9], which makes 2D materials very attractive both in fundamental studies and future electronic applications. Mechanical exfoliation method provides a “top-down” strategy to obtain high-quality 2D single crystals [10–12]. Most of the intrinsic properties are discovered on exfoliated 2D crystals, including the room-temperature quantum Hall effect [13] and twist

\* Corresponding author (email: liwei.liu@bit.edu.cn, l\_liu@pku.edu.cn, yhuang01@iphy.ac.cn)

† Huang X Y and Zhang L have the same contribution to this work.

angle induced superconductivity in graphene [14], and indirect to direct band gap transition in MoS<sub>2</sub>, WS<sub>2</sub>, etc. [3, 15]. After the first successful exfoliation of graphene in 2004 [16], mechanical exfoliation technique was regarded as a simple way to get 2D materials. In fact, even the mechanical exfoliation method is widely used to get high-quality 2D single crystals, the size of exfoliated flakes is always around few micrometers, which hinders further characterization and discovery of new 2D materials. For example, it is difficult to locate the position of micrometer size 2D materials and collect sufficient signal by the scanning tunneling microscopy (STM) and angle-resolved photoemission spectroscopy (ARPES). Besides, the small sized 2D samples cannot be used in integrated circuit devices.

In recent years, some researchers try to find new ways to improve the yield ratio and size of exfoliated 2D materials. Oxygen plasma treatment has been proved to be an effective way for exfoliating large area and high quality graphene and layered copper-based high temperature superconductors (Bi2212 etc.) [11]. Au-enhanced exfoliation has been used to get large area transition metal dichalcogenides (TMDCs), such as MoS<sub>2</sub>, WS<sub>2</sub> [17–19]. In our recent work, we extended the Au-enhanced exfoliation method to exfoliate more than 40 layered materials and provided a universal exfoliation routine [12], which will be widely used in the advanced studies for 2D materials. Our theoretical calculations indicate that the non-metallic elements in VA, VIA, and VIIA in periodic table of elements, such as P, As, S, Se, Te, Cl, have strong interaction with Au, and may form covalent-like quasi-bonding (CLQB) [12], which is relatively stronger than interlayer van der Waals interaction but still weaker than covalent bonds. Therefore, the Au film can improve the exfoliation yield ratio and flake size for those layered materials which containing the non-metallic elements above. Even the interlayer CLQB interaction has been demonstrated in black phosphorus, PtS<sub>2</sub>, PtSe<sub>2</sub> and CrS<sub>2</sub> [20–24], however, the CLQB interaction at the interface of layered materials and Au has not been reported in experimentally. So far, this 2D material-Au CLQB interaction is still not clear and difficult to be detected by some surface sensitive characterization tools, because the interaction is at the interface instead of the top surface of 2D materials. STM, ARPES and also X-ray photoelectron spectroscopy (XPS) cannot be easily used to unveil whether the covalent-like quasi-bonding exists at the interface. How to characterize this interaction is still a great challenge. Clarifying the existence of covalent-like quasi-bonding between Au and these 2D materials is not only important for examining the theoretical prediction, but also may provide some new clues to unveil the exfoliation mechanism and optimize exfoliation procedures to get wafer-scale large area 2D crystals.

As the prime nondestructive characterization tool, Raman spectroscopy has been widely used to identify the stacking order, strain field distribution, defects and layer numbers [25–27]. Different from the surface sensitive characterization tools, Raman spectroscopy can be applied to detect some information of 2D materials within a certain depth. Thus, Raman spectra may provide a new entry point to detect the CLQBs between Au and 2D materials. As reported in previous studies, most 2D materials consist of two kinds of Raman modes [28, 29], the in-plane vibrations and interlayer rigid vibrations, such as the interlayer shear (C) and layer breathing (LB) modes [30, 31]. In graphene system, the in-plane vibrations include D, G and 2D Raman peaks [29]. The C and LB modes in graphene and MoS<sub>2</sub> are sensitive to layer numbers and thus can be used to probe the interlayer information [28, 30].

MoS<sub>2</sub>, as one of the most well-studied 2D semiconductors, shows high on-off ratio in field-effect transistor and strong photoluminescence (PL), which has great potential in logic circuit, photon detector, and flexible/wearable devices [7, 8, 15]. The Raman spectra characters of monolayer and few layer MoS<sub>2</sub> have been well studied [28, 32], therefore, it is convenient to use MoS<sub>2</sub> as a reference to probe the CLQBs related behaviors by Raman spectroscopy. Here we report the low-frequency shear and breathing modes of few layer MoS<sub>2</sub> on different cases, including Au film, SiO<sub>2</sub>/Si and hole-array substrates. After comparing the Raman spectra of MoS<sub>2</sub> at low-frequency range, we demonstrate that the Au film can suppress the shear and breathing modes of MoS<sub>2</sub>, which provides a convincing evidence for the existence of CLQBs between Au-MoS<sub>2</sub> interface. This conclusion is further verified on few layer WS<sub>2</sub>, which show similar behaviors, indicating that the CLQBs at the interface of Au-TMDCs are a universal phenomenon.

## 2 Results and discussion

Few layer MoS<sub>2</sub> samples are exfoliated from bulk MoS<sub>2</sub> crystal through a newly developed Au-enhanced exfoliation method, which has been thoroughly introduced in our previous work [12]. Two metal layers (Au/Ti: 5 nm/2 nm) are deposited on Si substrates with 300 nm SiO<sub>2</sub> layer by electron-beam evaporation system. The flakes with different layer numbers can be determined by optical contrast and atomic force

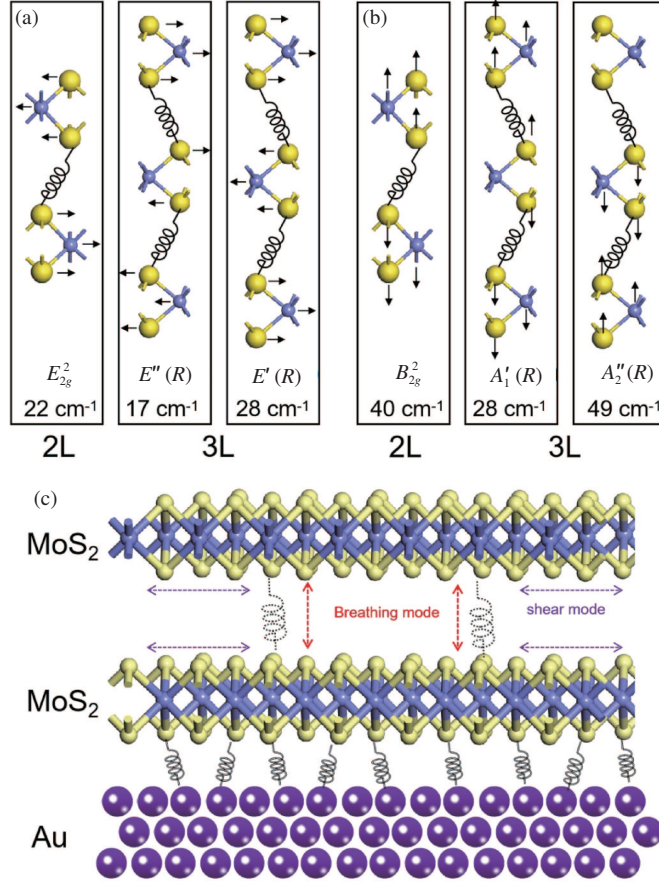


**Figure 1** (Color online) (a) Lattice structure and shear modes in 2L and 3L MoS<sub>2</sub>. (b) Layer breathing modes in 2L and 3L MoS<sub>2</sub>. The theoretical Raman peak positions of these modes based on the diatomic chain model are indicated. (c) Schematic image of bi-layer MoS<sub>2</sub> on Au film. The interaction between S atom and Au atom is indicated. The Au-S interaction can affect the shear mode and layer breathing mode of MoS<sub>2</sub> layers near the interface.

microscopy [32]. Raman measurements are performed using a WITec alpha300R system with a low-frequency detection capability ( $> 7 \text{ cm}^{-1}$ ). The excitation wavelength is 532 nm from a diode-pumped solid-state laser. In order to protect the sample, we set the laser power at 2 mW for all the measured spectra. The spectral resolution is  $\sim 0.4 \text{ cm}^{-1}$ , which facilitates to observe the fine peaks at low-frequency range.

There are 18 normal vibration modes for bulk MoS<sub>2</sub> and 2L-MoS<sub>2</sub> [33]. The two modes,  $A_{1g}$  ( $\sim 408 \text{ cm}^{-1}$  in bulk and  $\sim 405$  in 2L-MoS<sub>2</sub>) and  $E_{2g}^1$  ( $\sim 382 \text{ cm}^{-1}$  in bulk and  $\sim 383 \text{ cm}^{-1}$  in 2L), are observed when the laser is normal to the flake basal plane. These two modes are widely used to identify the layer number of MoS<sub>2</sub> ( $< 10\text{L}$ ) [32]. In low-frequency range, the doubly degenerate  $E_{2g}$  mode,  $E_{2g}^2$ , and one  $B_{2g}$  mode,  $B_{2g}^2$ , are shear and LB modes.  $E_{2g}^2$  is a rigid-layer vibration parallel to each unit MoS<sub>2</sub> layer (C mode), while  $B_{2g}^2$  corresponds to rigid-layer vibration perpendicular to each MoS<sub>2</sub> plane (LB mode). Different from even layer MoS<sub>2</sub>, which belong to  $D_{6h}$  point group, the odd layers, such as 1L and 3L-MoS<sub>2</sub> correspond to  $D_{3h}$  point group [34], with  $A_1'$  and  $A_2''$  belong to LB modes, and  $E'$  and  $E''$  belong to C modes. The origin of each vibration mode has been clearly presented in Tan's work [28], which will be used as reference in our experiments discussed below. The rigid-vibration modes of 2L and 3L are shown in Figures 1(a) and (b) schematically.

CLQB is a kind of non-covalent interaction with typical interaction energies of  $\sim 0.5 \text{ eV}$  per unit cell, which has been reported in recent theoretical studies [20, 21, 35]. The intermediate interaction energy for CLQB is a balance of a reasonably large Pauli repulsion induced by interlayer wavefunction overlap and an enhanced dispersion attraction caused by more pronounced electron correlation in 2D layers with high polarizability. The materials for CLQB with 2D crystals contain elements whose Fermi level falls in a partially filled band with mostly  $s$ - or  $p$ -electrons to prevent disrupting the electronic structure of

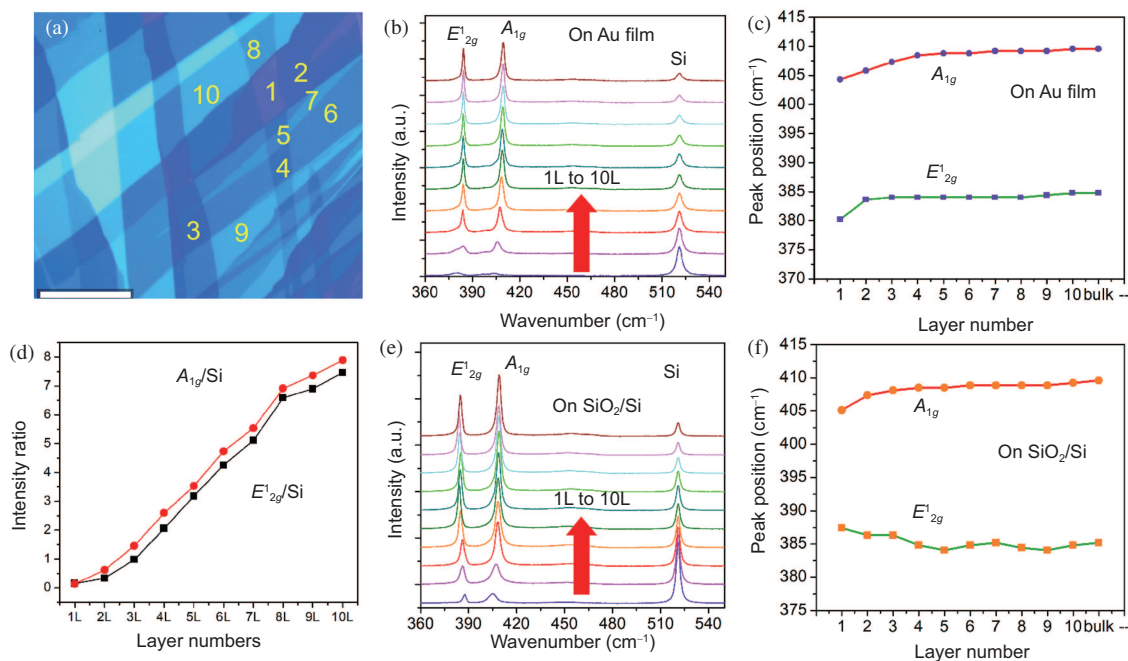


**Figure 2** (Color online) Raman spectra of MoS<sub>2</sub> exfoliated on Au film and after transferring onto SiO<sub>2</sub>/Si. (a) An optical image of MoS<sub>2</sub> flake exfoliated on Au film. The layer numbers are labeled on the flake. (b) and (e) are Raman spectra of 1L–10L MoS<sub>2</sub> (bottom up) on Au film and after transferring onto SiO<sub>2</sub>/Si substrate. The Raman peak of Si is used as reference. (c) and (f) are the statistic of A<sub>1g</sub> and E<sub>2g</sub><sup>1</sup> peak positions of 1L–10L and bulk MoS<sub>2</sub>, which are exfoliated on Au film and transferring onto SiO<sub>2</sub>/Si substrate, respectively. (d) The relative intensity ratio of A<sub>1g</sub> and E<sub>2g</sub><sup>1</sup> modes for 1L–10L MoS<sub>2</sub>.

2D layers, and which have highly polarizable electron densities to ensure a large dispersion attraction. Gold is a potential candidate to form CLQB with many layered materials, which has been proved to be useful to exfoliate many monolayer materials [12]. However, direct experimental evidence to prove the CLQB at Au-2D material interface is still lacking. We speculate that if CLQB exists between Au and 2D materials, the Raman spectra of 2D materials may deliver some clues, especially for shear and breathing vibration modes at the low-frequency range. The CLQB can induce pinning-effect and decrease the Raman intensity because the Au atoms is much heavier than S and Mo atoms. The pinning-effect of Au is schematically shown in Figure 1(c).

To uncover the CLQB induced effects for 2D materials, firstly, we measure the Raman spectra of few layer MoS<sub>2</sub> on Au/Ti/SiO<sub>2</sub>/Si substrate at higher frequency range, as shown in Figure 2. One MoS<sub>2</sub> flake with various thickness can be seen in Figure 2(a), and the layer numbers from 1L to 10L are labeled in the optical image. In Figure 2(b), the Raman spectra measured on 1L to 10L MoS<sub>2</sub> are presented, together with the peaks of Si at 521 cm<sup>-1</sup>. Both A<sub>1g</sub> and E<sub>2g</sub><sup>1</sup> can be observed on each layer. The position of the two peaks is summarized in Figure 2(c). For monolayer MoS<sub>2</sub>, the E<sub>2g</sub><sup>1</sup> peak is at 380 cm<sup>-1</sup>, which is a little lower than previous reported results [28,32]. As *N* increases, the intensities of the two main peaks increase while the intensity of Si getting weak gradually. After subtracting the background intensity, we plot the intensity ratio of A<sub>1g</sub>/Si and E<sub>2g</sub><sup>1</sup>/Si as a function of layer numbers, as shown in Figure 2(d). The layer number dependence of intensity ratio is almost linear within 10L. Therefore, one can determine the layer number by using the relative intensity ratio. In our previous work, we also proved the effectiveness of this method for determining the layer number of SnS<sub>2</sub> [36].

By spin-coating one layer of PMMA and etching the Au film by KI/I<sub>2</sub> solvent, the exfoliated MoS<sub>2</sub> flakes on Au film can be transferred onto arbitrary substrates. Raman spectra are measured on the same flake in Figure 2(a) after transferring from Au film to SiO<sub>2</sub>/Si. Detailed transfer process can be found in [12]. All the Raman spectra measurement parameters are the same before and after transfer. Similar to the results plotted in Figures 2(b) and (c), the spectra and two peaks position of MoS<sub>2</sub> (1L–10L) on SiO<sub>2</sub>/Si are presented in Figures 2(e) and (f). The intensities of two peaks, A<sub>1g</sub> and E<sub>2g</sub><sup>1</sup>, are all increasing after removing Au layer, indicating that the in-plane vibration of MoS<sub>2</sub> on Au film is suppressed. More detailed comparison can be seen in Figure 3, which show the two dominant peaks intensities of 1L and 2L MoS<sub>2</sub> before and after removing Au layer. The two peaks of 1L and 2L MoS<sub>2</sub> on Au film, A<sub>1g</sub> and E<sub>2g</sub><sup>1</sup>,

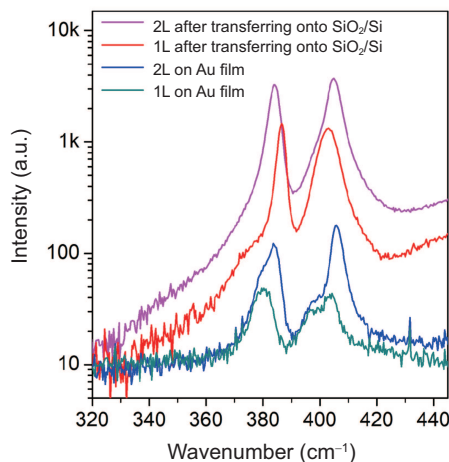


**Figure 3** (Color online) The two dominant Raman peaks ( $A_{1g}$  and  $E_{2g}^1$ ) of 1L and 2L MoS<sub>2</sub> exfoliated on Au film and after transferring onto SiO<sub>2</sub>/Si substrate.

show shoulders at low-frequency part. We believe this split is also closely related to the CLQB interaction at the Au/MoS<sub>2</sub> interface. There are 3 layers of atom in each MoS<sub>2</sub> unit layer, S-Mo-S, and once the bottom S atoms are pinned by Au atoms, the lattice vibration frequency between the two S layers will be different, both for the perpendicular ( $A_{1g}$ ) or parallel ( $E_{2g}^1$ ) vibration. Therefore, the peaks will split into higher frequency ones and normal ones. This is another evidence that CLQB exists between MoS<sub>2</sub> and Au, while there is no strong CLQB between SiO<sub>2</sub> and MoS<sub>2</sub>. The peak positions of  $A_{1g}$  mode for 1L–10L MoS<sub>2</sub> do not show obvious difference for the substrate with and without Au film. However, the  $E_{2g}^1$  mode shows different  $N$  dependence after transferring onto SiO<sub>2</sub>/Si. The  $E_{2g}^1$  peak positions for 1L–3L MoS<sub>2</sub> on Au film are 380.2, 383.6 and 384.0 cm<sup>-1</sup>, while these values for the same flake (1L–3L) after removing Au film and transferring onto SiO<sub>2</sub>/Si are 387.4, 386.3 and 386.3 cm<sup>-1</sup>. For monolayer, the peak position moves 7.2 cm<sup>-1</sup> to high-wavenumber direction after transferring. This Raman behavior of MoS<sub>2</sub> on Au film is similar to the MoS<sub>2</sub> and graphene under tensile strain [26, 37], which clearly demonstrates there must be some new interaction between Au and MoS<sub>2</sub>.

Even the SiO<sub>2</sub>/Si substrate shows weak interaction with MoS<sub>2</sub>, but it still cannot completely exclude the substrate induced effects. Since the low-frequency Raman modes are usually weaker than the main peaks at high-frequency range, the substrate can still suppress the rigid-layer vibration modes. Theoretically, suspended samples can completely remove substrate induced effects. To prepare suspended MoS<sub>2</sub> samples with different thickness, the SiO<sub>2</sub>/Si substrate is pre-patterned with hole-array before exfoliation. The diameter of each hole is 4 μm, fabricated by optical lithography patterning (Suss MicroTec GmbH, MA6) and plasma etching (Oxford, Plasma Pro 100 Cobra). Similar to the exfoliation process on normal flat substrates, we deposit Au/Ti metals on hole-array substrate before putting MoS<sub>2</sub> bulk crystal onto it.

Figure 4(a) shows the high-frequency Raman spectra of 1L–10L suspended MoS<sub>2</sub>, which is consistent with previous studies [28, 32]. The inset in Figure 4(a) is the optical image of one few layer MoS<sub>2</sub> flake exfoliated on hole array substrate, and the layer numbers (1L–5L) are labeled. Low-frequency Raman spectra of 1L–10 L MoS<sub>2</sub> are measured on this sample, which are shown in Figures 4(b) and (c) for the supported and suspended area, respectively. Since monolayer MoS<sub>2</sub> cannot show shear and breathing vibration modes, we just compare the low-frequency Raman spectra of MoS<sub>2</sub> with thickness larger than 2L. Two peaks are detected on suspended bilayer MoS<sub>2</sub> (Figure 4(c)), positioning at 22.3 and 38.4 cm<sup>-1</sup>. However, it is difficult to observe any peak for bilayer MoS<sub>2</sub> on Au film (Figure 4(b)). For 3L MoS<sub>2</sub> on Au film, two peaks of shear and breathing modes start to emerge on Au film (17.0 and 28.1 cm<sup>-1</sup>), but still with low intensity. There are four peaks detected on suspended 3L MoS<sub>2</sub> (16.3, 22.5, 28.8 and 39.2 cm<sup>-1</sup>). In previous reports, only one broad peak (~28 cm<sup>-1</sup>) was observed for 3L MoS<sub>2</sub> exfoliated on SiO<sub>2</sub>/Si [28, 38]. There are some small peaks in low-frequency range for samples on hole, especially for the 1L and 6L–10L. This phenomenon may be due to the interference of incident and reflected laser from hole's side and bottom, but not dependent on layer number of MoS<sub>2</sub>. Our results indicate that the suspended areas are more easily to observe low-frequency vibration modes since both surfaces are not confined by any solid materials, which show great advantages to study the shear and breathing modes of 2D materials in the future.

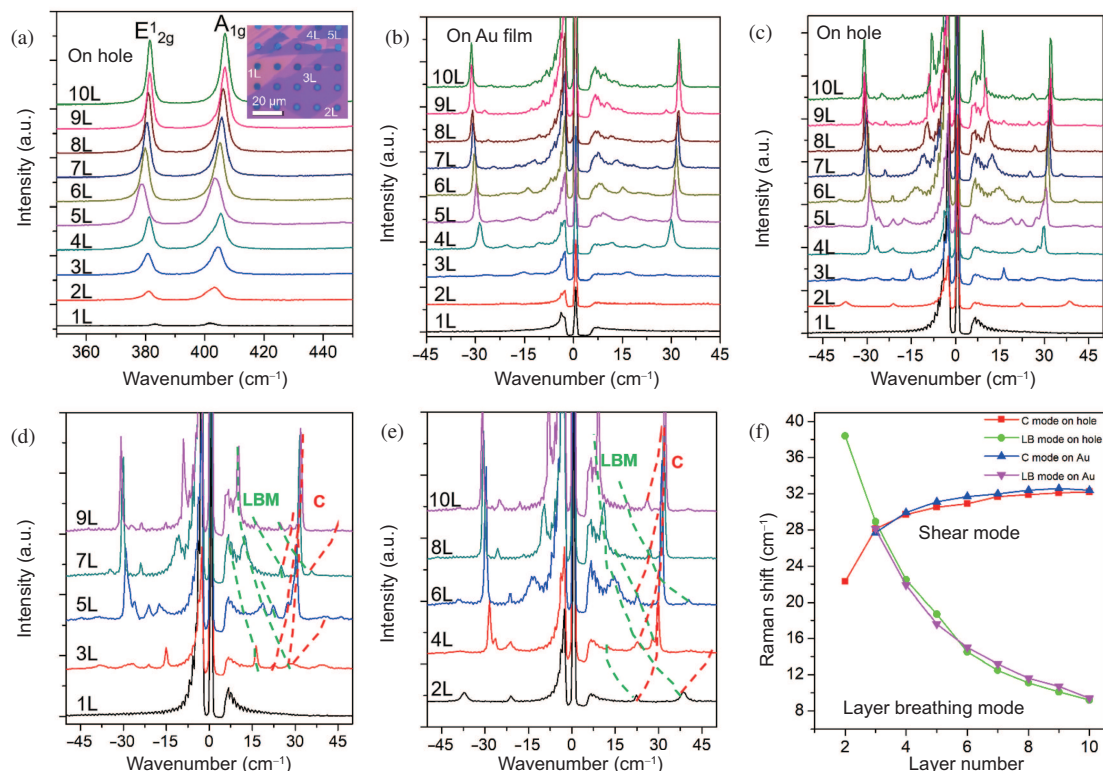


**Figure 4** (Color online) Low-frequency Raman spectra of few layer MoS<sub>2</sub>. (a) Raman spectra of 1L–10L suspended MoS<sub>2</sub>. The top-right inset is the optical image of MoS<sub>2</sub> onto hole array substrate, and the layer numbers from monolayer to 5L are labeled in this image. (b) and (c) are low-frequency Raman spectra of 1L–10L MoS<sub>2</sub> measure on supported areas and suspended hole areas, respectively. (d) and (e) are Stokes and anti-Stokes Raman spectra of odd (d) and even (e) number layer MoS<sub>2</sub> in the low-frequency range (–45 to 45 cm<sup>–1</sup>). The layer breathing modes and shear modes are indicated by green and red dashed lines. (f) Position of layer breathing and shear modes as a function of layer number. The data points for 2L MoS<sub>2</sub> on Au film are not shown since the main low-frequency modes is hard to distinguish.

The dominant shear mode of MoS<sub>2</sub> ( $\sim 30$  cm<sup>–1</sup>) on Au film becomes clearer as the thickness larger than 4L. However, the breathing modes are still weak even for 10L MoS<sub>2</sub> on Au film. On suspended areas, the intensities of both shear and breathing modes are getting enhanced as layer number increasing. Some new low-frequency peaks are observed for the first time, which again proves that the suspended samples are the most ideal ones for studying the rigid-layer vibration modes. For example, there are six Raman active modes for 5L from a theoretical point of view, but only three of them are observed in previous experimental results. In our 5L suspended MoS<sub>2</sub>, we directly observe all the six Raman modes at 18.7, 22.3, 27.3, 30.4, 40.8, and 45.9 cm<sup>–1</sup>, which is consistent with theoretical prediction [28].

As mentioned above, odd layer and even layer belong to  $D_{3h}$  and  $D_{6h}$  point groups [34], respectively. Thus, we plot the Raman spectra of 1L–10L suspended MoS<sub>2</sub> into two groups, as shown in Figures 4(d) and (e). The C and LB modes in each  $N$  are labeled by red and green dashed lines. As  $N$  increases, the C mode moves from lower wavenumber to higher wavenumber, while the LB mode moves from higher to lower wavenumber. Comparing to previous studies [28, 38], we find more low-frequency modes on suspended samples, which indicates that more rigid vibration modes are active on suspended structure since no substrate blocks the vibrations. The peak positions of both shear and layer breathing modes are summarized in Figure 4(f). The LB peak decreases from 38.4 cm<sup>–1</sup> on bilayer to 9.3 cm<sup>–1</sup> on 10L, while the C peak increases from 22.2 cm<sup>–1</sup> to 32.2 cm<sup>–1</sup>. These layer dependence behaviors of the two modes are consistent with previous reports [28, 38]. By comparing the low-frequency Raman spectra of few layer MoS<sub>2</sub> measured on Au film and suspended area, we find that both C and LB modes are becoming weak, especially the interlayer breathing modes. Low-frequency modes are not detectable on bilayer MoS<sub>2</sub> exfoliated on Au film, while the two modes can be clearly observed on suspended bilayer MoS<sub>2</sub>. More fine peaks in low-frequency range are detectable on suspended few layer MoS<sub>2</sub>. For example, we detected 4 peaks on 3L suspended MoS<sub>2</sub>, while only 1 broad peak was discovered on 3L MoS<sub>2</sub> exfoliated on SiO<sub>2</sub>/Si substrate in previous reports [28, 38]. Interestingly, the positions of main C and LB modes for MoS<sub>2</sub> on

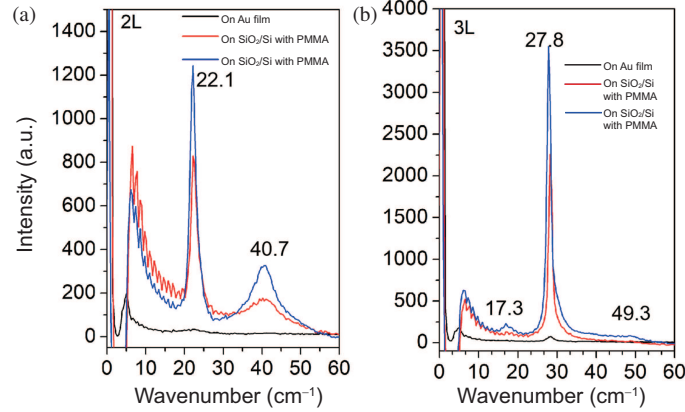


**Figure 5** (Color online) Raman spectra of bilayer (a) and tri-layer (b) MoS<sub>2</sub> in low-frequency range. The black, red and blue curves are measured on the same 2L and 3L flakes exfoliated on Au film, after transferring onto SiO<sub>2</sub>/Si with PMMA and after removing PMMA, respectively. All the Raman spectra are measured using the same parameters.

**Table 1** Statistics of main low-frequency peak intensity of 2L to 5L MoS<sub>2</sub> (0–60 cm<sup>-1</sup>)<sup>a)</sup>

Layer number	Peak position	On Au film	After transfer with PMMA	After transfer without PMMA
2L	22.1	17.9	822.7	1244.5
3L	27.8	61.0	2255.7	3553.3
4L	22.8	52.4	1333.6	1771.2
5L	19.3	78.7	1561.2	2050.8

a) As can be seen in the table, the Raman intensity of MoS<sub>2</sub> on Au film is the lowest for one specific layer number, while the dramatically increase after removing Au layer and transferring onto SiO<sub>2</sub>/Si.

Au film and hole are almost the same for  $L > 3$ , as shown in the statistic curves in Figure 4(f). The Raman results demonstrate that the interaction between MoS<sub>2</sub> and Au shows clear an-isotropic, which is consistent with the pinning-effect as we speculated above. The Raman spectra of few layer MoS<sub>2</sub> on Au provide a clear evidence to confirm the existence of CLQB at the interface.

To further verify the CLQB induced pinning-effect, we measure Raman spectra of bilayer and tri-layer MoS<sub>2</sub> on Au film, encapsulated between PMMA/SiO<sub>2</sub> and removing PMMA. As shown in Figure 5(a), the Raman spectrum of bilayer MoS<sub>2</sub> on Au is difficult to detect any peaks. But the two peaks are quite clear after removing Au layer and transferring onto SiO<sub>2</sub>/Si substrate. The intensities of the two peaks at 22.1 and 40.7 cm<sup>-1</sup> increase slightly after removing PMMA, which indicates no strong coupling between MoS<sub>2</sub> and SiO<sub>2</sub> or PMMA. Similar behavior can be discovered on tri-layer MoS<sub>2</sub>, as shown in Figure 5(b). After deducing the background signal, we summarize the main peak intensity at low-frequency of 2L to 5L MoS<sub>2</sub> in Table 1. For example, the intensity of 3L MoS<sub>2</sub> at 27.8 cm<sup>-1</sup> is 61, while this value increases to 2255.7 after etching Au and transferring onto SiO<sub>2</sub>/Si. The intensity further increases to 3553.3 after removing PMMA, which has been enhanced about 5.8 times than the peak intensity measured on Au film.

In order to verify the pinning-effect in other few layer 2D materials, we exfoliate WS<sub>2</sub> on hole-array substrate and measure Raman spectra as reference. As shown in Figure 6(a), the shear mode of WS<sub>2</sub> on Au can be observed as thickness larger than 3L, but LB mode is difficult to detect even for 10L WS<sub>2</sub>. However, these Raman peaks at low-frequency range can be clearly detected for the suspended few layer WS<sub>2</sub> (Figure 6(b)). This phenomenon is consistent with the one observed on MoS<sub>2</sub>/Au system, which demonstrates the CLQB induced pinning-effect is universal for 2D materials exfoliated on Au film.

### 3 Conclusion and perspective

The Raman spectra of few layer MoS<sub>2</sub> are measured on Au film and after removing Au layer on SiO<sub>2</sub>/Si substrate. For the in-plane vibration modes, we find the  $E_{2g}^1$  peak at 380.2 cm<sup>-1</sup> for monolayer MoS<sub>2</sub> on Au film, which moves to 387.4 cm<sup>-1</sup> after moving Au film and transferring onto Si substrate. Few layer MoS<sub>2</sub> flakes are further exfoliated on hole array substrate by using the Au-enhanced exfoliation method. The MoS<sub>2</sub> flakes on hole areas are free-standing, which can completely exclude substrate-induced effects.

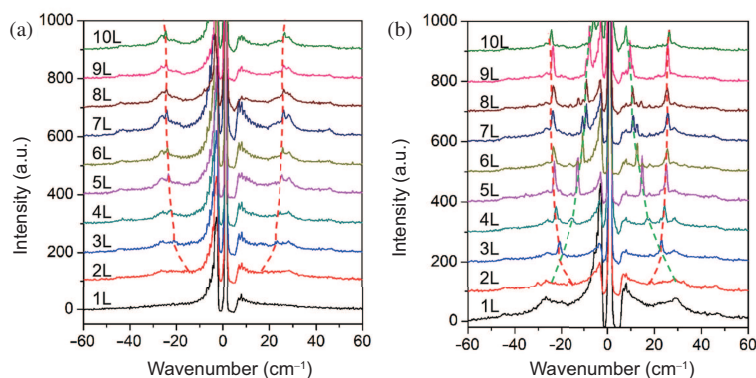


**Figure 6** (Color online) Low-frequency Raman spectra of 1L–10L WS<sub>2</sub> measure on supported areas (a) and suspended hole areas (b).

Therefore, the Raman spectra of few layer MoS<sub>2</sub> measured on hole area provide an ideal reference to understand the Raman behavior of MoS<sub>2</sub> on other solid substrates. Both C and LB modes are clearly observed on suspended few layer MoS<sub>2</sub>, and some of the vibration modes are discovered for the first time. The intensity of low-frequency modes of few layer MoS<sub>2</sub> on Au film is suppressed, especially for the breathing modes. After removing MoS<sub>2</sub> flakes from Au film and transferring onto SiO<sub>2</sub>/Si substrates, the intensities of C and LB modes are dramatically enhanced. The suppression of low-frequency modes of few layer MoS<sub>2</sub>, which is exfoliated on Au film, is attributed to the pinning-effect induced by CLQB at the interface of Au and MoS<sub>2</sub>. This pinning-effect is further verified on WS<sub>2</sub> samples, which is also exfoliated on the hole-array substrate.

The interaction between 2D materials and different substrate surfaces plays an important role for exfoliation and modification of the properties of 2D materials. Among many solid surfaces underneath 2D materials, Au is the special one because it has a stronger interaction with S, Se, Te, P, As, Cl, Br, I atoms. These non-metallic atoms are mainly the out-most elements in many layered materials, such as MX<sub>2</sub> (M = Mo, W, Ta, Nb, Sn, X = S, Se, Te), black phosphorus, RuCl<sub>3</sub>, CrBr<sub>3</sub>, and CrI<sub>3</sub>. Here, our findings have revealed the existence of CLQB between 2D materials and Au, providing a direct evidence in experimental. After investigating the mechanism of low-frequency modes of MoS<sub>2</sub>, we speculate that there must be some pinning-effect for few layer MoS<sub>2</sub> if CLQB generates between MoS<sub>2</sub> and Au. These results indicate that the pinning-effect is commonly seen in few layer 2D materials prepared by the Au-enhanced exfoliation. This work also demonstrates that the suspended 2D crystals show great advantage for Raman studies and may present unique potential in other optical and electrical measurements in the future.

**Acknowledgements** This work was supported by National Key Research and Development Program of China (Grant Nos. 2019YFA0308000, 2018YFA0704201, 2019YFA0307801), National Natural Science Foundation of China (Grants Nos. 11874405, 62022089, 61971035, 61725107, 11974001, U1932153), Youth Innovation Promotion Association of CAS (Grants No. 2019007), Beijing Natural Science Foundation (Grants Nos. 2192022, Z190011), and Strategic Priority Research Program (B) of the Chinese Academy of Sciences (Grant No. XDB33000000). We thank Prof. Ping-Heng TAN and Dr. Miaoling LIN for discussion and valuable comments.

## References

- Dai Z H, Liu L Q, Zhang Z. Strain engineering of 2D materials: issues and opportunities at the interface. *Adv Mater*, 2019, 31: 1805417
- Wang B, Li Z C, Wang C H, et al. Folding large graphene-on-polymer films yields laminated composites with enhanced mechanical performance. *Adv Mater*, 2018, 30: 1707449
- Mak K F, Lee C, Hone J, et al. Atomically thin MoS<sub>2</sub>: a new direct-gap semiconductor. *Phys Rev Lett*, 2010, 105: 136805
- Álvarez-Pérez G, Folland T G, Errea I, et al. Infrared permittivity of the biaxial van der waals semiconductor alpha-MoO<sub>3</sub> from near- and far-field correlative studies. *Adv Mater*, 2020, 32: 1908176
- Neto A H C, Guinea F, Peres N M R, et al. The electronic properties of graphene. *Rev Mod Phys*, 2009, 81: 109–162
- Qin S Y, Kim J, Niu Q, et al. Superconductivity at the two-dimensional limit. *Science*, 2009, 324: 1314–1317
- Radisavljevic B, Radenovic A, Brivio J, et al. Single-layer MoS<sub>2</sub> transistors. *Nat Nanotech*, 2011, 6: 147–150
- Li N, Wang Q Q, Shen C, et al. Large-scale flexible and transparent electronics based on monolayer molybdenum disulfide field-effect transistors. *Nat Electron*, 2020, 3: 711–717
- Yu H, Liao M Z, Zhao W J, et al. Wafer-scale growth and transfer of highly-oriented monolayer MoS<sub>2</sub> continuous films. *ACS Nano*, 2017, 11: 12001–12007
- Novoselov K S, Geim A K, Morozov S V, et al. Two-dimensional gas of massless Dirac fermions in graphene. *Nature*, 2005, 438: 197–200

- 11 Huang Y, Sutter E, Shi N N, et al. Reliable exfoliation of large-area high-quality flakes of graphene and other two-dimensional materials. *ACS Nano*, 2015, 9: 10612–10620
- 12 Huang Y, Pan Y H, Yang R, et al. Universal mechanical exfoliation of large-area 2D crystals. *Nat Commun*, 2020, 11: 2453
- 13 Novoselov K S, Jiang Z, Zhang Y, et al. Room-temperature quantum hall effect in graphene. *Science*, 2007, 315: 1379
- 14 Cao Y, Fatemi V, Fang S, et al. Unconventional superconductivity in magic-angle graphene superlattices. *Nature*, 2018, 556: 43–50
- 15 Zhao W J, Ribeiro R M, Toh M L, et al. Origin of indirect optical transitions in few-layer MoS<sub>2</sub>, WS<sub>2</sub>, and WSe<sub>2</sub>. *Nano Lett*, 2013, 13: 5627–5634
- 16 Novoselov K S, Geim A K, Morozov S V, et al. Electric field effect in atomically thin carbon films. *Science*, 2004, 306: 666–669
- 17 Velický M, Donnelly G E, Hendren W R, et al. Mechanism of gold-assisted exfoliation of centimeter-sized transition-metal dichalcogenide monolayers. *ACS Nano*, 2018, 12: 10463–10472
- 18 Magda G Z, Peto J, Dobrik G, et al. Exfoliation of large-area transition metal chalcogenide single layers. *Sci Rep*, 2015, 5: 14714
- 19 Desai S B, Madhvapathy S R, Amani M, et al. Gold-mediated exfoliation of ultralarge optoelectronically-perfect monolayers. *Adv Mater*, 2016, 28: 4053–4058
- 20 Qiao J S, Kong X H, Hu Z X, et al. High-mobility transport anisotropy and linear dichroism in few-layer black phosphorus. *Nat Commun*, 2014, 5: 4475
- 21 Hu Z X, Kong X H, Qiao J S, et al. Interlayer electronic hybridization leads to exceptional thickness-dependent vibrational properties in few-layer black phosphorus. *Nanoscale*, 2016, 8: 2740–2750
- 22 Zhao Y D, Qiao J S, Yu P, et al. Extraordinarily strong interlayer interaction in 2D layered PtS<sub>2</sub>. *Adv Mater*, 2016, 28: 2399–2407
- 23 Zhao Y D, Qiao J S, Yu Z, et al. High-electron-mobility and air-stable 2D layered PtSe<sub>2</sub> FETs. *Adv Mater*, 2017, 29: 1604230
- 24 Wang C, Zhou X Y, Pan Y H, et al. Layer and doping tunable ferromagnetic order in two-dimensional CrS<sub>2</sub> layers. *Phys Rev B*, 2018, 97: 245409
- 25 Hao Y, Wang Y, Wang L, et al. Probing layer number and stacking order of few-layer graphene by raman spectroscopy. *Small*, 2010, 6: 195–200
- 26 Huang Y, Wang X, Zhang X, et al. Raman spectral band oscillations in large graphene bubbles. *Phys Rev Lett*, 2018, 120: 186104
- 27 Cañado L G, Jorio A, Ferreira E H M, et al. Quantifying defects in graphene via raman spectroscopy at different excitation energies. *Nano Lett*, 2011, 11: 3190–3196
- 28 Zhang X, Han W P, Wu J B, et al. Raman spectroscopy of shear and layer breathing modes in multilayer MoS<sub>2</sub>. *Phys Rev B*, 2013, 87: 115413
- 29 Ferrari A C. Raman spectroscopy of graphene and graphite: disorder, electron phonon coupling, doping and nonadiabatic effects. *Solid State Commun*, 2007, 143: 47–57
- 30 Tan P H, Han W P, Zhao W J, et al. The shear mode of multilayer graphene. *Nat Mater*, 2012, 11: 294–300
- 31 Lui C H, Malard L M, Kim S H, et al. Observation of layer-breathing mode vibrations in few-layer graphene through combination raman scattering. *Nano Lett*, 2012, 12: 5539–5544
- 32 Li H, Zhang Q, Yap C C R, et al. From bulk to monolayer MoS<sub>2</sub>: evolution of Raman scattering. *Adv Funct Mater*, 2012, 22: 1385–1390
- 33 Sandoval S J, Yang D, Frindt R F, et al. Raman study and lattice dynamics of single molecular layers of MoS<sub>2</sub>. *Phys Rev B*, 1991, 44: 3955–3962
- 34 Molina-Sánchez A, Wirtz L. Phonons in single-layer and few-layer MoS<sub>2</sub> and WS<sub>2</sub>. *Phys Rev B*, 2011, 84: 155413
- 35 Qiao J S, Pan Y H, Yang F, et al. Few-layer tellurium: one-dimensional-like layered elementary semiconductor with striking physical properties. *Sci Bull*, 2018, 63: 159–168
- 36 Huang Y, Sutter E, Sadowski J T, et al. Tin disulfide—an emerging layered metal dichalcogenide semiconductor: materials properties and device characteristics. *ACS Nano*, 2014, 8: 10743–10755
- 37 Ni Z H, Yu T, Lu Y H, et al. Uniaxial strain on graphene: Raman spectroscopy study and band-gap opening. *ACS Nano*, 2008, 2: 2301–2305
- 38 Zeng H L, Zhu B R, Liu K, et al. Low-frequency Raman modes and electronic excitations in atomically thin MoS<sub>2</sub> films. *Phys Rev B*, 2012, 86: 241301